PHYSICAL REVIEW B **79**, 140503(R) (2009)

Doping dependence of the gap anisotropy of the high-temperature $YBa_2Cu_3O_{7-\delta}$ superconductor

K. Nakayama,[1] T. Sato,[1] K. Terashima,[1] T. Arakane,[1] T. Takahashi,[1,2] M. Kubota,[3] K. Ono,[3] T. Nishizaki,[4] Y. Takahashi,[4] and N. Kobayashi[4]

[1]*Department of Physics, Tohoku University, Sendai 980-8578, Japan*

[2]*WPI Research Center, Advanced Institute for Materials Research, Tohoku University, Sendai 980-8577, Japan*

[3]*Institute of Materials Structure Science, KEK, Tsukuba 305-0801, Japan*

[4]*Institute for Materials Research, Tohoku University, Sendai 980-8577, Japan*

(Received 4 December 2008; published 14 April 2009)

We have performed high-resolution angle-resolved photoemission spectroscopy of $YBa_2Cu_3O_{7-\delta}$ with various hole concentrations from under-to-optimal doping. We have determined the momentum dependence of bulk superconducting gap as a function of hole concentration and found the enhancement of antinodal gap, the deviation from simple $d_{x^2-y^2}$ wave, and the reduction of superconducting coherence weight in the underdoped region. We also found the universality of the doping dependence of the SC-gap size and symmetry in bilayered cuprates. These results suggest the importance of the long-range pairing interactions in the underdoped region.

DOI: 10.1103/PhysRevB.79.140503 PACS number(s): 74.72.Bk, 71.18.+y, 74.25.Jb, 79.60.−i

Angle-resolved photoemission spectroscopy (ARPES) has revealed the key electronic structure of high-temperature superconductors (HTSC) (Ref. 1) by the unique capability to directly observe the momentum-resolved electronic states. Intensive ARPES measurements have revealed the opening of a $d_{x^2-y^2}$-wave-like superconducting (SC) gap in $Bi_2Sr_2CaCu_2O_8$ (Bi2212),[2,3] while the essential character of SC-gap symmetry is still controversial due to the presence of inhomogeneities, oxygen vacancies,[4] and pseudogap.[5,6] For instance, the substantial deviation from a simple $d_{x^2-y^2}$ wave was recently reported for single-layered $Bi_2Sr_2CuO_6$ (Ref. 7) and $La_{2-x}Sr_xCuO_4$ (LSCO),[8] suggesting a possible crystal structure or T_c dependence of the low-energy excitation properties. In this regard, $YBa_2Cu_3O_{7-\delta}$ (Y123) is an ideal candidate since the crystal structure is distinctly different from that of Bi- and La-based cuprates. While Y123 is a bilayered system with the maximum T_c comparable to that of Bi2212, there is a marked difference in the T_c vs doping relation between Bi2212 and Y123. Unlike Bi2212, the T_c value of Y123 shows a plateau at 60 K in underdoped (UD) region around 1/8 doping like in single-layered LSCO, although the origin of this plateau is still highly controversial.[9–11] It is thus particularly important to elucidate the bulk electronic states of Y123, not only to clarify the universality of electronic states of HTSC but also to obtain an insight into the relation between the low-energy excitation properties and the characteristic T_c variation of UD Y123. However, an ARPES study of bulk electronic states of Y123 has been difficult due to the contamination from the CuO-chain band and the presence of surface states.[1] Indeed, the first convincing evidence for the SC-gap opening was reported by Lu *et al.*[12] in 2001, while the detailed momentum dependence of the SC gap and the microscopic origin of surface states have not been fully understood yet. More recent ARPES studies[13,14] clarified the overall bulk- and surface-band dispersions as well as the $d_{x^2-y^2}$-wave-like SC-gap opening in nearly optimally doped and overdoped Y123, concluding that the surface state arises from the heavily overdoped CuO_2 planes near the surface. Although these studies provided important insights into the electronic states of Y123, the evolution of electronic states upon hole doping is still unclear at present.

In this Rapid Communication, we report high-resolution ARPES results of Y123 with various hole concentrations from UD to optimally doped (OP) region, including the 60-K plateau region. By extracting the bulk electronic states with circularly polarized photons of synchrotron radiation, we have succeeded in observing the bilayer splitting of bulk bands even in the UD sample in addition to the reduction in the SC coherence weight. We also found that the maximal size of the SC gap and the gap anisotropy show a significant variation in doping, providing an evidence for the universality of the anisotropic low-energy excitation gap in bilayered HTSC. We discuss implications of the present experimental results in relation to the characteristic phase diagram of Y123.

High-quality single crystals of naturally untwinned $YBa_2Cu_3O_{7-\delta}$ (Y123; δ=0.4, 0.2, and 0.06) were grown by the self-flux method using yttria crucibles. The oxygen concentration was controlled by annealing the samples under oxygen or nitrogen atmosphere at high temperature.[15] The T_c of samples was determined by the magnetic susceptibility measurement as 60, 80, and 92 K for δ=0.4, 0.2, and 0.06, respectively. We call these samples as UD60K, UD80K, and OP92K samples, respectively. ARPES measurements have been done using a VG-SCIENTA SES2002 spectrometer at BL28A beamline in Photon Factory, Tsukuba. We used circularly polarized 46-eV photons to excite photoelectrons. The energy and angular resolutions were set at 12–25 meV and 0.2°, respectively. The sample orientation was determined by the Laue x-ray diffraction prior to ARPES measurements. A clean surface was obtained by *in situ* cleaving of crystals in an ultrahigh vacuum of 1×10^{-10} Torr. The sample was kept at 10 K during measurements except for temperature-dependent experiments. The Fermi level (E_F) of samples was referenced to that of a gold film evaporated onto the sample substrate.

Figure 1 shows the plot of ARPES intensity at E_F as a function of two-dimensional wave vector around ΓY cut for [Fig. 1(a)] UD60K, [Fig. 1(b)] UD80K, and [Fig. 1(c)] OP92K Y123 samples. As most clearly seen in the OP92K sample [Fig. 1(c)], there are two large Fermi surfaces (FSs) (solid green curves) centered at S point in the Brillouin zone (BZ). Similar FS are also recognized in UD60K and UD80K

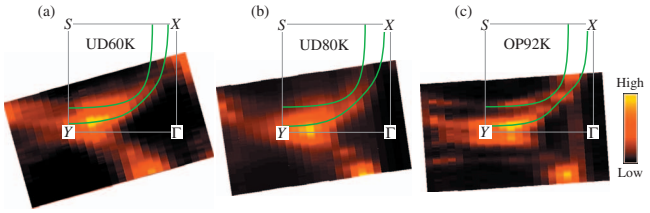

FIG. 1. (Color) Plot of ARPES intensity at E_F as a function of two-dimensional wave vector measured at 10 K with 46-eV photons for (a) UD60K, (b) UD80K, and (c) OP92K Y123. ARPES intensity is integrated over the energy range of 30 meV centered at E_F. Green curves are guide lines for the FS of surface bands obtained by smoothly connecting determined k_F points.

samples although the ARPES-intensity distribution looks gradually broadened with less doping. The hole concentration (p) estimated from the average volume of two FSs is 0.27 ± 0.02, 0.29 ± 0.02, and 0.29 ± 0.02 for UD60K, UD80K, and OP92K samples, respectively. The invariance of hole concentration, as also reported in the previous ARPES study,[14] suggests that the observed FSs are attributed to the surface bonding and antibonding bands of the overdoped topmost CuO_2 bilayer.[13]

Figure 2 shows the ARPES-intensity plot as a function of binding energy and wave vector for [Fig. 2(a)] UD60K, [Fig. 2(b)] UD80K, and [Fig. 2(c)] OP92K samples, measured at 10 K along several cuts (shown by arrows in [Fig. 2(d)]) in the off-nodal region located midway between the node and antinode. In all the samples, we find a couple of bands (indicated by open circles) which are ascribed to the surface bonding and antibonding bands to form the large FS shown

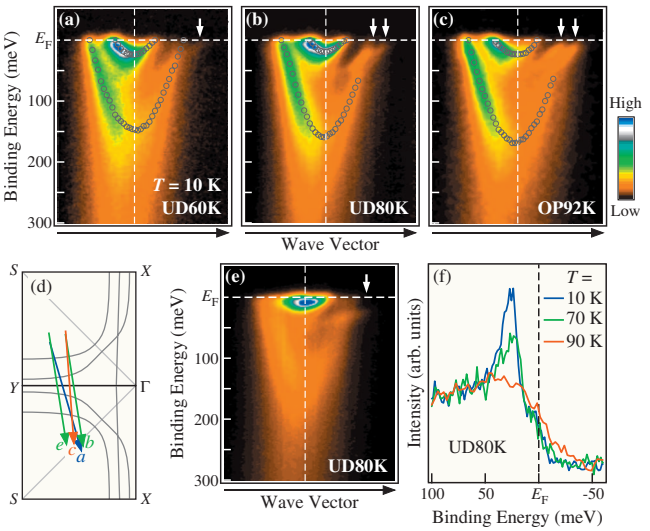

FIG. 2. (Color) Plot of ARPES intensity as a function of binding energy and wave vector for (a) UD60K, (b) UD80K, and (c) OP92K Y123, measured at 10 K along cuts shown by arrows in (d). Open circles show the surface-band dispersions determined from the peak position in ARPES spectrum divided by the FD function. White arrows show the k_F positions for bulk bands. (e) Same as (b) except for measured cut [cut e in (d)]. (f) Temperature dependence of ARPES spectrum of UD80K sample measured at the k_F point indicated by a white arrow in (e).

in Fig. 1. Although the surface-band dispersion is almost symmetric with respect to the ΓY high symmetry line, the spectral intensity appears quite asymmetric with respect to the ΓY line contrary to the symmetric intensity measured with linearly polarized light.[14] This is due to the strong matrix-element effect since it is expected that the variation in the vector potential of incident circularly polarized photons at the crystal surface leads to a circular dichorism for the surface states.[16] Thus the observed asymmetric intensity supports the surface origin of these bands. In the right half of BZ in Figs. 2(a)–2(c), where the photoemission intensity of surface bands is significantly suppressed due to the circular polarization, we find two additional bands with the energy dispersion distinctly different from that of the surface bands in contrast to the ARPES result with linearly polarized light.[14] These two bands have been assigned to the bulk bands originating in the CuO_2 planes.[13] It is remarked that the bilayer splitting of the bulk band is clearly seen even in the UD80K sample as in the OP92K sample, although it is not clearly resolved in the UD60K sample. This indicates that the coherence between two CuO_2 planes in a unit cell is still well established even in the UD sample with the T_c value as low as 80 K. Figure 2(e) shows the ARPES-intensity plot of UD80K sample at 10 K measured at cut e, closer to the antinode than cut b. As compared to cut b, the intensity of bulk band at E_F is substantially suppressed due to opening of a larger SC gap in cut e. Furthermore, the bulk-band dispersion looks more flattened, reflecting the stronger quasiparticle (QP) mass-renormalization effect near the antinode.[13,14] To elucidate the character of this QP band in more detail, we measured the temperature dependence of ARPES spectrum at the Fermi-vector (k_F) point, and the result is shown in Fig. 2(f). At 10 K, a well-defined sharp QP peak is observed at 25 meV, and the midpoint of the leading edge is shifted toward higher binding energy due to the SC-gap opening. Upon increasing the temperature, the QP peak and the leading-edge gap are still clearly seen even at 70 K slightly below T_c (80 K), while the peak completely disappears and the gap almost closes at 90 K, indicating that the peak is assigned as the bulk SC coherence peak.

To clarify the doping dependence of the SC-gap symmetry, we determined the k_F position of the bulk bands for three samples with different doping levels. As seen in Fig. 3(a), the FS volume monotonically decreases with less doping indicative of the bulk nature of these bands, in contrast to the almost doping-independent nature of FS volume of the surface states (Fig. 1). Figures 3(b)–3(d) show ARPES spectra measured at 10 K at various k_F points of the bulk band. We regarded the ARPES spectrum away from the k_F point as the background[17,18] and subtracted it from each k_F spectrum to highlight the intrinsic bulk SC peak. In all the samples, the energy position of bulk SC peak, which basically corresponds to the SC-gap size, is strongly k dependent and is gradually weakened with approaching the node [ϕ=45°, where ϕ is the Fermi surface angle defined in Fig. 3(a)], showing the overall $d_{x^2-y^2}$-like order parameter. We find a Fermi-edge structure due to the surface band in the antinodal region ($\phi \sim 0°$), which is well separated from the bulk QP peak and therefore does not affect the estimation of the SC-gap size. The intensity of the QP peak is systematically re-

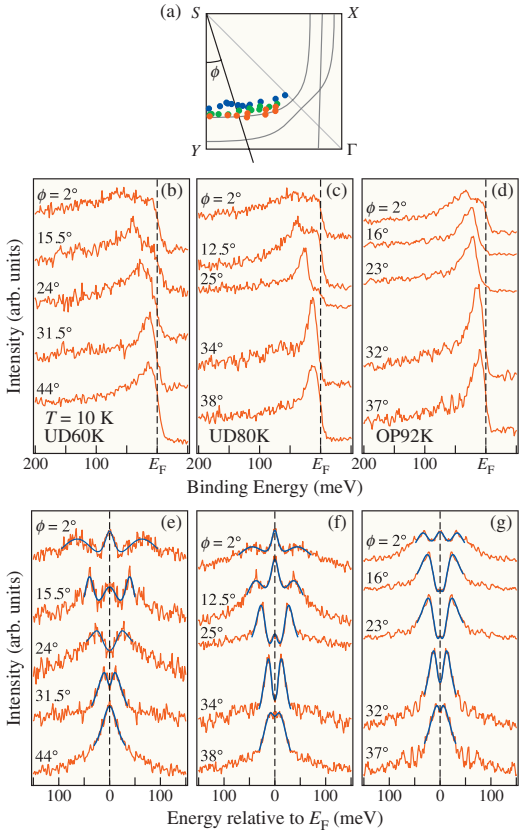

FIG. 3. (Color) (a) Location of k_F points of the bulk bands for UD60K (blue circles), UD80K (green), and OP92K (red) samples together with the definition of FS angle (ϕ). (b)–(d) ARPES spectra after subtracting the background at 10 K measured at various k_F points of bulk bands for (b) UD60K, (c) UD80K, and (d) OP92K Y123 samples. FS angle (ϕ) defined in the inset is indicated on each spectrum. (e)–(g) Symmetrized spectra of (b)–(d). Blue curves show the results of numerical fittings by the phenomenological spectral function (Ref. 6) and an additional Lorentzian peak at E_F which accounts for the surface states.

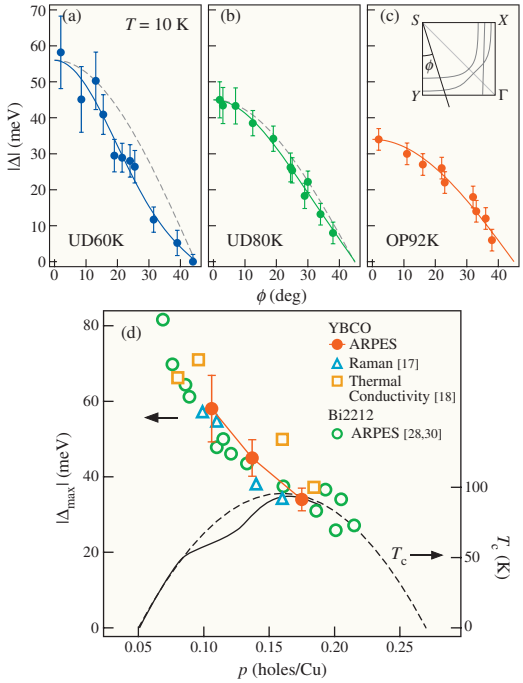

FIG. 4. (Color) Momentum (FS angle, ϕ) dependence of SC-gap size at 10 K for (a) UD60K, (b) UD80K, and (c) OP92K Y123 samples. Dashed gray lines show the energy gap for an ideal $d_{x^2-y^2}$ symmetry case while solid colored lines are the fitting results with the gap function of $\Delta=\Delta_{\max}(B\cos 2\phi+(1-B)\cos 6\phi)$ (Ref. 29). In OP92K sample, both lines coincide with each other. (d) Doping dependence of the antinodal SC-gap size determined by present ARPES (red circles), compared with results from the B_{1g} Raman scattering (Ref. 22) (blue triangles) and the thermal conductivity (Ref. 23) (yellow square) experiments of Y123 and previous ARPES experiments of Bi2212 (Refs. 28 and 30) (green circles). Solid black line shows the doping (p) vs T_c curve obtained for Y123 (Ref. 34) while the dashed line represents a proposed "ideal" p vs T_c curve (Ref. 35).

duced from the OP92K sample to UD60K sample, showing a close relationship between the superfluid density and T_c.[19] To estimate the SC-gap size, we have symmetrized ARPES spectra and performed numerical fittings as shown in Figs. 3(e)–3(g). At first, we folded each k_F spectrum with respect to E_F and then added it to the unfolded spectrum. This method is useful to remove the effect of the Fermi-Dirac (FD) distribution function.[6] After this symmetrization procedure, we fit each symmetrized spectrum with the phenomenological spectral function[6] and an additional Lorentzian peak at E_F which accounts for the metallic surface component. In addition to the overall $d_{x^2-y^2}$-like feature of the gap for all the samples, it is remarked that a clear node ($\Delta=0$) is observed at around $\phi=45°$ in the UD60K sample.[20] This suggests that the mixture of s-wave component as reported in overdoped samples[21] is less possible in the underdoped samples.

In Figs. 4(a)–4(c), we show the size of SC gap as a function of ϕ for three samples. In the antinodal region where the SC gap shows a maximal value, the gap size systematically increases with reducing the hole concentration from OP92K to UD60K. We plot in the phase diagram of Fig. 4(d) the antinodal-gap size determined in the present ARPES in comparison with the gap values reported from the B_{1g} Raman scattering[22] and the thermal conductivity[23] measurements of Y123. All the data show a good quantitative agreement in the doping dependence of gap, demonstrating the general trend of the larger gap in the more underdoped sample. It is also remarked that the k dependence of SC gap in the OP92K sample is well reproduced by the ideal $d_{x^2-y^2}$ gap function while a finite deviation is recognized in the UD60K and UD80K samples.

Next we discuss the bulk electronic structure of Y123 in comparison with Bi2212. In UD Y123 samples, we observed (i) the bilayer band splitting, (ii) the reduction of the SC coherence peak, (iii) the enhancement of the antinodal-gap size, and (iv) the deviation from the ideal $d_{x^2-y^2}$-wave symmetry of the SC gap. These characteristic features are qualitatively similar to previous ARPES reports on Bi2212,[24–30] suggesting the universality in the doping dependence of electronic states near E_F. As shown in Fig. 4(d), the doping dependence of the antinodal-gap size in Y123 coincides well with that of Bi2212,[1,27–30] although the T_c vs doping relation

is substantially different in the UD region between two compounds. The observed larger SC-gap size in the underdoped region would be caused by the stronger pairing interactions. We also found close similarity in the evolution of the gap anisotropy between Y123 and Bi2212. To characterize the anisotropy, we have performed numerical fittings with $\Delta(\phi)=\Delta_0[B\cos(2\phi)+(1-B)\cos(6\phi)]$,[29] where the second term represents the higher harmonic of the $d_{x^2-y^2}$-wave gap function. As shown in Figs. 4(a)–4(c), the k dependence of the SC gap in Y123 is satisfactorily fit with the parameter values of $B=0.85$, 0.95, and 1.0 for UD60K, UD80K, and OP92K samples, respectively. This variation in B value with doping shows a quantitatively good agreement with that of Bi2212,[29] demonstrating the close similarity in the doping dependence of the SC gap and its anisotropy between Y123 and Bi2212. These results suggest the importance of long-range interactions for the pairing in the underdoped region in both Bi2212 and Y123.[29] It is noted here that while we have revealed the close similarities of the low-energy excitations between Y123 and Bi2212, the previous ARPES study by Lu *et al.*[12] reported a large in-plane anisotropy of the SC gap in Y123 which does not exist in Bi2212. This suggests that the interference from the CuO-chain band should be taken into account to elucidate the intrinsic character of the SC gap in Y123. It is also remarked that it is essential to extract the SC-gap value from the spectrum just at the k_F point since the small deviation from the k_F point causes a marked difference in the estimated SC-gap size due to a sizable dispersion of the QP peak even around the antinode.

Finally, we discuss implications of the present ARPES results in relation to the characteristic phase diagram of Y123. Recently, it has been reported that the Δ_{max} value of $La_{2-x}Ba_xCuO_4$ (LBCO) shows a local maximum at the 1/8 doping,[31] where the T_c is suddenly reduced to zero and the formation of static spin/charge stripes has been proposed.[32] This observation suggests the anticorrelation between Δ_{max} and T_c around the 1/8 doping region in LBCO. By considering the argument that the 60-K plateau in Y123 corresponds to the 1/8 anomaly in La-based HTSC,[10,11,33,34] one may expect an enhancement of Δ_{max} also in Y123 in the 60-K plateau region. If it is the case, the Δ_{max} of Y123 would be larger than that of Bi2212 in this doping region since the 1/8 anomaly has not been observed in pristine Bi2212. However, as seen in Fig. 4(d), no clear difference in the Δ_{max} value between Y123 and Bi2212 is observed in the 1/8 doping region, suggesting that the anticorrelation behavior between Δ_{max} and T_c is very weak in Y123.

In summary, we have performed high-resolution synchrotron radiation ARPES on $YBa_2Cu_3O_{7-\delta}$ with various hole concentrations. We have succeeded in directly observing the bulk-band dispersions by the merit of the circularly polarized synchrotron radiation and determined the doping evolution of k dependence of the SC gap. We found several anomalies in the underdoped region, such as the enhancement of the antinodal SC gap and the substantial deviation from the $d_{x^2-y^2}$-wave gap symmetry suggestive of the importance of strong long-range pairing interactions. The present ARPES results demonstrate the universality of low-energy excitation gap in bilayered HTSC.

This work was supported by grants from JST-CREST and MEXT of Japan. The work at KEK-PF was done under the approval of Photon Factory Program Advisory Committee (Proposal No. 2006S2-001) at the Institute of Material Structure Science, KEK. K.N. and K.T. thank JSPS for financial support.

[1] A. Damascelli, Z. Hussain, and Z.-X. Shen, Rev. Mod. Phys. **75**, 473 (2003).
[2] Z.-X. Shen *et al.*, Phys. Rev. Lett. **70**, 1553 (1993).
[3] H. Ding, M. R. Norman, J. C. Campuzano, M. Randeria, A. F. Bellman, T. Yokoya, T. Takahashi, T. Mochiku, and K. Kadowaki, Phys. Rev. B **54**, R9678 (1996).
[4] G. Deutscher, Rev. Mod. Phys. **77**, 109 (2005).
[5] A. G. Loeser *et al.*, Science **273**, 325 (1996).
[6] M. R. Norman *et al.*, Nature (London) **392**, 157 (1998).
[7] T. Kondo, T. Takeuchi, A. Kaminski, S. Tsuda, and S. Shin, Phys. Rev. Lett. **98**, 267004 (2007).
[8] K. Terashima, H. Matsui, T. Sato, T. Takahashi, M. Kofu, and K. Hirota, Phys. Rev. Lett. **99**, 017003 (2007).
[9] B. W. Veal and A. P. Paulikas, Physica C **184**, 321 (1991).
[10] J. L. Tallon *et al.*, Physica C **282-287**, 236 (1997).
[11] M. Akoshima and Y. Koike, J. Phys. Soc. Jpn. **67**, 3653 (1998).
[12] D. H. Lu *et al.*, Phys. Rev. Lett. **86**, 4370 (2001).
[13] K. Nakayama, T. Sato, K. Terashima, H. Matsui, T. Takahashi, M. Kubota, K. Ono, T. Nishizaki, Y. Takahashi, and N. Kobayashi, Phys. Rev. B **75**, 014513 (2007).
[14] V. B. Zabolotnyy *et al.*, Phys. Rev. B **76**, 064519 (2007).
[15] T. Nishizaki, Y. Takahashi, and N. Kobayashi, Physica C **468**, 664 (2008).
[16] V. B. Zabolotnyy *et al.*, Phys. Rev. B **76**, 024502 (2007).
[17] A. Kaminski *et al.*, Phys. Rev. B **69**, 212509 (2004).
[18] M. Platé *et al.*, Phys. Rev. Lett. **95**, 077001 (2005).
[19] Y. J. Uemura *et al.*, Phys. Rev. Lett. **62**, 2317 (1989).
[20] It is difficult to determine the SC-gap size of bulk bands near $\phi=45°$ on UD80K and OP92K samples since bulk and surface bands are too close to each other.
[21] N.-C. Yeh *et al.*, Phys. Rev. Lett. **87**, 087003 (2001).
[22] S. Sugai, H. Suzuki, Y. Takayanagi, T. Hosokawa, and N. Hayamizu, Phys. Rev. B **68**, 184504 (2003).
[23] M. Sutherland *et al.*, Phys. Rev. B **67**, 174520 (2003).
[24] Y. D. Chuang, A. D. Gromko, A. V. Fedorov, Y. Aiura, K. Oka, Y. Ando, M. Lindroos, R. S. Markiewicz, A. Bansil, and D. S. Dessau, Phys. Rev. B **69**, 094515 (2004).
[25] D. L. Feng *et al.*, Phys. Rev. B **65**, 220501(R) (2002).
[26] D. L. Feng *et al.*, Science **289**, 277 (2000).
[27] H. Ding, J. R. Engelbrecht, Z. Wang, J. C. Campuzano, S. C. Wang, H. B. Yang, R. Rogan, T. Takahashi, K. Kadowaki, and D. G. Hinks, Phys. Rev. Lett. **87**, 227001 (2001).
[28] J. C. Campuzano *et al.*, Phys. Rev. Lett. **83**, 3709 (1999).
[29] J. Mesot *et al.*, Phys. Rev. Lett. **83**, 840 (1999).
[30] K. Tanaka *et al.*, Science **314**, 1910 (2006).
[31] T. Valla *et al.*, Science **314**, 1914 (2006).
[32] J. M. Tranquada *et al.*, Nature (London) **429**, 534 (2004).
[33] Y. Ando and K. Segawa, Phys. Rev. Lett. **88**, 167005 (2002).
[34] R. Liang, D. A. Bonn, and W. N. Hardy, Phys. Rev. B **73**, 180505(R) (2006).
[35] M. R. Presland *et al.*, Physica C **176**, 95 (1991).